Journal of Organometallic Chemistry, 394 (1990) 433–454
Elsevier Sequoia S.A., Lausanne
JOM 21127

Reaction of $Ru_3\{\mu$-H, μ-O=CNMe$_2\}(CO)_{10}$ with diarylacetylenes; synthesis and subsequent reaction of a $\{\mu$-carboxamido, μ-σ,π-vinyl$\}$-hexacarbonyl diruthenium complex with propyne. Crystal and molecular structures of $Ru_2\{\mu$-O=CNMe$_2$,μ-σ,π-C(p-tol)=CH(p-tol)$\}(CO)_6$, and of $Ru_2\{\mu$-O=CNMe$_2$,μ-σ,π-C(CH$_3$)=C(H)-C(p-tolyl)=CH(p-tolyl)$\}(CO)_6$ (p-tol = p-CH$_3$C$_6$H$_4$) *

W. Krone-Schmidt, W.J. Sieber, N.M. Boag, C.B. Knobler and H.D. Kaesz[*]
Department of Chemistry and Biochemistry, University of California, Los Angeles, CA 90024-1569 (U.S.A.)

(Received March 22nd, 1990; in revised form May 22nd, 1990)

Abstract

The complex $Ru_3\{\mu$-O=CNMe$_2$,μ-H$\}(CO)_{10}$ (**1**) is observed to react with diphenylacetylene (**2a**), di(p-tolyl)acetylene (**2b**), or di(p-anisyl)acetylene (**2c**), at 23° C in hexane solution over a period of 12 h to give $Ru_2\{\mu$-O=CNMe$_2$,μ-σ,π-C(Ar)=CH(Ar)$\}(CO)_6$, Ar = Ph (**3a**), p-CH$_3$C$_6$H$_4$ (**3b**), or p-CH$_3$OC$_6$H$_4$ (**3c**). Principal by-products are $Ru_3(CO)_{12}$ and the acetylene oligomerization complexes $\{\eta^5$-(OC)$_3$RuC(Ar)=C(Ar)C(Ar)=C(Ar)$\}$Ru(CO)$_3$, Ar = C$_6$H$_5$ (**4a**), Ar = p-tolyl, CH$_3$C$_6$H$_4$ (**4b**), Ar = p-anisyl, CH$_3$OC$_6$H$_4$ (**4c**). Variable temperature ^{13}C NMR of **3a**, **3b**, and **3c** indicates the presence of two rapidly interconverting isomers in solution, one with *geminal* and the other with *vicinal* bridging groups. Complex **3b** is observed to react with propyne at 23° C in hexane over a period of 4 h giving as principal product $Ru_2\{\mu$-O=CNMe$_2$,μ-σ,π-C(CH$_3$)=C(H)C(p-tolyl)CH(p-tolyl)$\}(CO)_6$, **5**.

The crystal and molecular structures of **3b** and **5** have been determined using graphite-monochromatized Mo-K_α radiation on a Huber four circle diffractometer under control of a VAX 11/750 computer. Complex **3b** crystallizes in the monoclinic space group $P2_1/a$; cell dimensions $a = 20.1744(23)$, $b = 7.3166(8)$, $c = 18.9413(22)$ Å, and $\beta = 93.2730(31)°$ and $Z = 4$, $V = 2786.12$ Å^3; ρ(calc.) = 1.55 g cm^{-3}. A total of 3923 unique reflections with $I > 3\sigma(I)$ were used in the refinement; final discrepancy indices, $R = 0.057$ and $R_w = 0.071$. The crystal consists of discrete molecules of the complex in which the metal–metal separation Ru(1)–Ru(2)

---

* Dedicated to Professor F.G.A. Stone on the occasion of his 65th birthday.

0022-328X/90/$03.50

= 2.739(1) Å. The two bridging groups, namely $\{\mu\text{-}\sigma,\pi\text{-}C(50)(Ar)=C(40)H(Ar)\}$ and $\{O(30)=C(30)NMe_2\}$, are seen to be attached to the two metal centers in a *vicinal* arrangement with a near octahedral arrangement of σ-bonded atoms around each metal. Bond distance parameters for the bridging groups are (Å): Ru(2)–O(30) = 2.117(5); O(30)–C(30) = 1.283(8); Ru(1)–C(30) = 2.106(7); Ru(1)–C(50) = 2.324(7); Ru(1)–C(40) = 1.410(9); Ru(2)–C(50) = 2.081(7); C(40)–C(50) = 1.410(9).

Complex **5** crystallizes in the monoclinic space group $P2_1/c$ with cell dimensions: $a = 10.421(4)$, $b = 33.157(10)$, $c = 8.896(3)$ Å, $\beta = 90.34(3)°$ and $Z = 4$, $V = 3078$ Å^3; $\rho(\text{calc.}) = 1.49$ g cm^{-3}. The structure was solved by the heavy atom method. A total of 3159 unique reflections with $I > 3\sigma(I)$ were used in the refinement; final discrepancy indices, $R_F = 0.085$ and $R_{wF} = 0.110$. Complex **5** consists of two tricarbonyl ruthenium fragments joined by a strong Ru–Ru bond, 2.726(2) Å, accompanied by a bridging carboxamido group and a bridging σ,π-group $(C(CH_3)=C(H)R$ ($R = C(p\text{-tolyl})=C(H)p\text{-tolyl}$) in a *sigma-geminal* arrangement. This type of complex is perceived as a common intermediate to the oligomerization products **4a**, **4b**, **4c** observed in the present and previous studies, and the complex $Ru_2\{\mu\text{-}O=CNMe_2, \mu\text{-}O=CC(Me)=CMe(\eta^2\text{-}CMe=CHMe)\}(CO)_5$, observed in a previous study.

Introduction

As described in a preceding paper [1a] attempts to prepare ruthenium or osmium cluster complexes containing a μ-σ,π-vinyl group by reaction of $M_3\{\mu\text{-}H,\mu\text{-}O=CNMe_2\}(CO)_{10}$ (M = Ru or Os) with but-2-yne led instead to trinuclear derivatives containing an η^3-allylic group as the principal product for M = Ru or as the exclusive product for M = Os. To avoid the 1,2-hydrogen shift leading to such η^3-allyl derivatives, we turned to diarylacetylenes whose reactions with $Ru_3\{\mu\text{-}H,\mu\text{-}O=CNMe_2\}(CO)_{10}$ (**1**) are described in this work [1b,c]. A companion work using ^{13}C-enriched diphenylacetylene and PPh_3-substituted derivatives has recently appeared [2].

The aryl acetylenes do not react with $Os_3\{\mu\text{-}H,\mu\text{-}O=CNMe_2\}(CO)_{10}$ up to 125 °C in octane, whereupon the known metallacyclic derivatives $\{\eta^5\text{-}(OC)_3\overline{OsC(Ph)=C(Ph)C(Ph)=C}(Ph)\}Os(CO)_3$, and $Os_3\{\mu\text{-}\eta^4\text{-}C(Ph)=C(Ph)\text{-}C(Ph)=C(Ph)\text{-}\}(CO)_9$ are obtained [3]. The σ,π-vinyl complexes $Os_3\{\mu\text{-}H,\mu\text{-}\sigma,\pi\text{-}CH=CH_2\}(CO)_{10}$ [4] and $Os_3\{\mu\text{-}H,\mu\text{-}\sigma,\pi\text{-}CPh=CHPh\}(CO)_{10}$ [5], have been obtained in the reaction of $Os_3\{\mu\text{-}H\}_2(CO)_{10}$ respectively with acetylene or diphenylacetylene.

Experimental

General information. Solvents and reagents were of commercial reagent grade and were dried and redistilled under nitrogen. The petroleum ether cited throughout this work is that from Mallinckrodt (Analytical Reagent, b.pt. 35–60 °C). Diphenylacetylene (**2a**) was obtained from the Aldrich Co. Di(p-tolyl)acetylene (**2b**) or di(p-anisyl)acetylene (**2c**) were prepared from 4,4′-dimethylbenzil and 4,4′-dimethoxybenzil (Aldrich), respectively, according to the method described for the

Table 1

IR carbonyl absorptions [a]

Compound [b]	Absorptions/cm^{-1}
3a	2080s, 2049vs, 2008s, 2002m, 1986m, 1981w, 1976w, 1507vw [c]
3b	2078s, 2048vs, 2008s, 2001m, 1985m, 1980w, 1975w, 1505vw [c]
3c	2077s, 2047vs, 2007s, 2000m, 1983m, 1980w, 1975w, 1508vw [c]
4a [d]	2081s, 2042vs, 2021s, 1997s, 1954w,br
4b	2079s, 2039vs, 2018s, 1995s, 1945w,br
4c	2077s, 2037vs, 2016s, 1991s, 1940w,br
5	2076s, 2047vs, 2010m, 2001vs, 1985m, 1972m, 1506vw [c]

[a] In spectrophotometric grade hexane. [b] See Scheme 1 for identification of compounds. [c] Bridging CO absorption. [d] The reported maxima are 2082s, 2043vs, 2020s, 1998vs, 1952w, cm^{-1} [8].

preparation of **2a** [6]. The starting complex $Ru_3\{\mu\text{-}H,\mu\text{-}O{=}CNMe_2\}(CO)_{10}$ was prepared according to the cited literature procedure [7].

Because some of the products in this work are not air stable, all manipulations including chromatographic separations were routinely carried out under a purified nitrogen atmosphere using Schlenk techniques. Carbonyl infrared spectra were recorded on a Nicolet MX-1 FT-IR spectrometer; data are summarized in Table 1. ^{1}H and ^{13}C NMR spectra were recorded on a JEOL FX90Q spectrometer; ^{1}H NMR spectra were calibrated against internal residual $CHCl_3$ at -7.25 ppm or tetramethylsilane (TMS). NMR data are given in Table 2. Fast atom bombardment mass spectra (FAB-MS) were obtained using a locally constructed FAB gun mounted on a modified AEI MS-9 double focusing mass spectrometer. A 6 keV xenon atom beam was used with gun tube current at 1 mA. One mg of compound is slurried into 1 μL of a liquid matrix composed of 9 parts of 18-crown-6 ether (Aldrich) to 1 part tetraglyme. A trace (0.2 μl) of Santovac-5 oil (Monsanto) is added before insertion

Table 2

NMR data

Compound	^{1}H [a] resonances, δ/ppm (m = multiplet; s = singlet)
3a [b]	7.15–6.82 (m, 10H), 4.64 (s, 1H), 3.12 (s, 3H), 2.76 (s, 3H)
3b [c]	7.19–6.76 (m, 10H), 4.63 (s, 1H), 3.17 (s, 3H), 2.80 (s, 3H), 2.22 (s, 3H), 2.15 (s, 3H)
3c [b]	7.23–6.39 (m), 4.62 (s, 1H), 3.71 (s, 6H) [d], 3.21 (s, 3H), 2.84 (s, 3H)
	$\{^{1}H\}^{13}C$ NMR [a,e] resonances, δ/ppm
3a [f]	204.9 (μ-O=*C*), 201.0, 199.3, 199.2, 196.5, 194.1 (CO), 193.1(C^{50}), 191.3 (CO), 152.1, 141.2 (*ipso*-Ar), 127.9, 127.5, 126.6, 124.4 (other Ar), 77.9 (C^{40}) [h], 40.8, 35.4 ($N(CH_3)_2$)
3b [f]	205.5 (μ-O=*C*), 201.5, 199.8, 199.6, 196.9, 194.7 (CO), 192.7 (C^{50}), 191.9 (CO), 150.2, 139.4 (*ipso*-Ar), 135.4, 135.2, 129.1, 128.4 (other Ar), 78.7 (C^{40}) [i], 40.9, 33.5 ($N(CH_3)_2$, 21.2 (CH_3Ph).
3c [b,d,g]	206.5 (μ-O=*C*), 200.0, 198.0, 195.6, 194.5 (CO), 192.2 (C^{50}), 189.2 (CO), 132.9 (*para*-Ar), 129.6, 129.3 (other Ar), 54.6 (CH_3OPh), 40.1, 34.8 ($N(CH_3)_2$)

[a] Referenced to internal $(CH_3)_4Si$ (1%). Resonances listed are for the major constituent in solution. [b] In $CDCl_3$. [c] In CD_2Cl_2. [d] Assignments are incomplete due to interference from peaks of **4c**. [e] In the presence of 20 mg $Cr(acac)_3$. [f] At -50 °C. [g] At 23 °C. [h] At +30 °C this peak merges with a resonance at 102.9 for the minor isomer to a single broad peak at 85.8. [i] At +30 °C this peak merges with a resonance at 103.1 for the minor isomer to a single broad peak at 87.5.

into the mass spectrometer. Calculated and observed multiplets are available in ref. 1b. Elemental analyses were performed by Schwarzkopf Laboratories, Inc.

*Reaction of PhC≡CPh (**2a**) with $Ru_3\{\mu$-H,μ-$O{=}CNMe_2\}(CO)_{10}$ (**1**).* To a quantity of **1** (1.00 g, 1.52 mmol) in 200 ml petroleum ether, is added 545 mg (3.05 mmol) of **2a** and the mixture stirred under a stream of N_2 at 23°C for 24 h. Solvent is reduced in volume to 30 ml in a rotary evaporator and is placed on a silica gel column (Baker Analyzed, 60–200 mesh; 2 cm dia. × 20 cm length). Four fractions are eluted. Starting with petroleum ether, a yellow band is eluted which contains $Ru_3(CO)_{12}$ (40 mg, 0.06 mmol) and excess **2a** (80 mg, 0.45 mmol). Continuing with petroleum ether/CH_2Cl_2 (9 : 1), an orange band consisting of unreacted **1** (85 mg, 0.13 mmol) is next eluted. With petroleum ether/CH_2Cl_2 (4 : 1) a yellow-orange band is eluted consisting of $Ru_2\{\mu$-$O{=}CNMe_2,\mu$-σ,π-$C(Ph){=}CHPh\}(CO)_6$ (**3a**) (415 mg, 0.67 mmol, yield: 48% based on unrecovered **1**). Product **3a** is obtained as a yellow oil. FAB/MS shows a multiplet for (parent ion − 2 CO) centered at 594

Table 3

Summary of crystal data collection and refinement parameters [a]

Compound	**3b** [b]	**5** [c]
Formula	$C_{25}H_{21}NO_7Ru_2$	$C_{28}H_{25}NO_7Ru_2$
Formula wt.	649.6	689.6
Space group	$P2_1/a$	$P2_1/c$
a/Å	20.1744(23)	10.421(4)
b/Å	7.3166(8)	33.157(10)
c/Å	18.9413(22)	8.896(3)
β/deg	93.2730(31)	90.34(3)
V/Å^3	2786.12	3078(1)
Z	4	4
ρ(calc.)/g cm^{-3}	1.55	1.49
Crystal size/mm^3	0.5 × 0.5 × 0.6	0.35 × 0.5 × 0.6
Indices of the faces	$(00\bar{1})(\bar{1}10)(\bar{1}00)$ $(100)(0\bar{1}0)(001)$' [d]	$(010)(100)(0\bar{1}0)$ $(\bar{1}00)(0\bar{3}\bar{1})(001)$ [e]
Abs. coeff (μ/cm^{-1})	10.993	10.281
Transmission factors	0.5252–0.5768	0.7501–0.9509
Scan rate/deg min^{-1}	6	4
Scan range: deg below $K_{\alpha 1}$	1.2	1.0
deg above $K_{\alpha 2}$	1.6	1.0
2θ limits/deg	$0 < 2\theta \leqslant 54$	$0 < 2\theta < 50$
Take off angle/deg	4.0	4.0
Observations	$+h, +k, \pm l$	$+h, +k, \pm l$
Total observed data	6,100	5459
Unique reflections ($I > 3\sigma(I)$)	3923	3159
Final no. of variables	316	273
Goodness of fit [f] (GOF)	2.05	2.92
R [g]	0.056	0.085
R_w [h]	0.066	0.110

[a] Radiation source, Mo-K_α = 0.71070 Å; temp = 23°C. [b] $Ru_2\{\mu$-$O{=}C(NMe_2),\mu$-σ,π-$C(p$-tolyl$){=}C(H)(p$-tolyl$)\}(CO)_6$. [c] $Ru_2\{\mu$-$O{=}C(NMe_2),\mu$-σ,π-$C(CH_3){=}C(H)C(p$-tolyl$){=}C(H)(p$-tolyl$)\}(CO)_6$. [d] Perpendicular distances from a common point of 0.0, 0.0, 0.0, 0.613, 0.516, and 0.613 mm, respectively. [e] Perpendicular distances from a common point of 0.0, 0.0, 0.35, 0.05, 0.0, and 0.6 mm, respectively. [f] $GOF = [\sigma w(|F_o| - |F_c|)^2/N_o - N_v)]^{\frac{1}{2}}$, where $w = 1/[\sigma(|F_o|)]^2$. [g] $R = \Sigma \| F_o| - |F_c \| / |F_o|$. [h] $R_w = [\Sigma w(|F_o| - |F_c|)^2/|F_o|/\Sigma w|F_o|^2]^{\frac{1}{2}}$.

(m.wt. of **3a** – 2 CO, 534). We independently confirm the presence of six CO groups through ^{13}C NMR, see Table 2. $C_{25}H_{21}NO_7Ru_2$ (649.59): calc. C 46.23, H 3.26, N 2.16; found C 45.92, H 3.53, N 2.29%.

The fourth band (yellow-brown), is eluted with CH_2Cl_2/petroleum ether (70 : 30). This fraction yields a yellow oil. IR absorptions identify this as the metallacyclic derivative $\{\eta^5\text{-(OC)}_3\overline{\text{RuC(Ph)=C(Ph)C(Ph)=C}}\text{(Ph)}\}\text{Ru(CO)}_3$, **4a** [8].

*Reaction of (p-tolyl)C≡C(p-tolyl) (**2b**) with $Ru_3\{\mu\text{-}H,\mu\text{-}O{=}CNMe_2\}(CO)_{10}$ (**1**).* To a quantity of **1** (1.00 g, 1.54 mmol) in 350 ml petroleum ether, is added **2b** (650 mg, 3.15 mmol) and the mixture is stirred under a stream of N_2 at 23°C for 24 h. Solvent volume is reduced to 30 ml in a rotary evaporator and the residue is placed on a silica gel column (Baker Analyzed, 60–200 mesh; 2 cm dia. × 20 cm length). Five fractions are eluted: starting with petroleum ether, a yellow band is obtained

Table 4

Final atomic positional parameters for $Ru_2\{\mu\text{-}O{=}CNMe_2,\mu\text{-}\sigma,\pi\text{-}C(p\text{-tolyl}){=}CH(p\text{-tolyl})\}(CO)_6$, **3b**

Atom	*x*	*y*	*z*
C(11)	0.96351(45)	0.53426(119)	0.73572(49)
C(12)	0.84449(45)	0.68947(117)	0.76727(46)
C(13)	0.92392(44)	0.60639(122)	0.88805(49)
C(21)	0.75509(41)	0.39431(116)	0.91214(37)
C(22)	0.86541(40)	0.26766(102)	0.97996(43)
C(23)	0.77696(44)	0.03501(120)	0.89266(44)
C(30)	0.94992(34)	0.25518(100)	0.84485(39)
C(31)	1.03916(42)	0.05881(135)	0.89350(51)
C(32)	1.06592(44)	0.36913(146)	0.85353(56)
C(40)	0.85287(33)	0.25385(88)	0.72677(36)
C(41)	0.84394(34)	0.27381(100)	0.64810(37)
C(42)	0.82090(47)	0.42593(125)	0.61485(43)
C(43)	0.81322(48)	0.43560(134)	0.54072(45)
C(44)	0.82937(46)	0.28909(133)	0.49956(43)
C(45)	0.85183(50)	0.13541(134)	0.53371(48)
C(46)	0.86130(40)	0.12597(115)	0.60779(42)
C(47)	0.82115(65)	0.29713(168)	0.41871(52)
C(50)	0.80503(33)	0.29904(91)	0.77532(37)
C(51)	0.73681(34)	0.35557(100)	0.74729(36)
C(52)	0.70279(37)	0.51414(102)	0.76559(40)
C(53)	0.63774(43)	0.54510(121)	0.73932(49)
C(54)	0.60392(38)	0.42615(136)	0.69583(49)
C(55)	0.63605(41)	0.26423(127)	0.67896(49)
C(56)	0.70255(39)	0.22961(111)	0.70379(45)
C(57)	0.53301(48)	0.45805(168)	0.66984(65)
N(30)	1.01483(30)	0.23110(91)	0.86106(37)
O(11)	1.00176(38)	0.56159(110)	0.69619(42)
O(12)	0.81900(34)	0.81918(81)	0.74608(36)
O(13)	0.94050(38)	0.67880(102)	0.93802(38)
O(21)	0.71292(33)	0.47429(94)	0.93454(32)
O(22)	0.89160(32)	0.28042(91)	1.03464(34)
O(23)	0.74468(43)	−0.09337(108)	0.89388(43)
O(30)	0.91311(23)	0.11665(66)	0.85658(26)
Ru(01)	0.89731(3)	0.48173(8)	0.80189(3)
Ru(02)	0.82529(3)	0.25327(8)	0.88275(3)

which contains $Ru_3(CO)_{12}$, (40 mg, 0.06 mmol, 6%) and excess **2b** (100 mg, 0.48 mmol). Continuing with petroleum ether/CH_2Cl_2 (9 : 1), an orange band is obtained consisting of unreacted **1** (200 mg, 0.30 mmol). This is closely followed by **4b** (50 mg, 0.06 mmol, 6%). With petroleum ether/CH_2Cl_2 (4 : 1) a yellow-orange band is eluted consisting of $Ru_2(\mu\text{-O=CNMe}_2,\mu\text{-}\sigma,\pi\text{-C(}p\text{-tolyl)=CH(}p\text{-tolyl)\}(CO)}_6$, **3b**, (415 mg, 0.67 mmol). Yield: 70% based on unrecovered **1**. Product **3b** is obtained as a yellow oil. It can be crystallized from CH_2Cl_2, but suitable crystals for X-ray studies are obtained from a hexane/CH_2Cl_2 mixture. FAB-MS shows a multiplet for (parent ion −1 CO) centered at 622 (m.wt. of **3b** − 1 CO). We independently confirm the presence of six CO groups through ^{13}C NMR, see Table 2.

Table 5

Final atomic positional parameters for $Ru_2\{\mu\text{-O=CNMe}_2,\mu\text{-}\sigma,\pi\text{-C(CH}_3\text{)=C(H)C(}p\text{-tolyl)=CH(}p\text{-tolyl)\}(CO)}_6$, **5**

Atom	*x*	*y*	*z*
C(11)	−0.3767(18)	−0.1332(8)	1.0446(22)
C(12)	−0.5435(18)	−0.0800(7)	0.8839(20)
C(13)	−0.3706(18)	−0.0464(6)	1.0758(22)
C(21)	−0.1597(16)	−0.0326(6)	0.5021(19)
C(22)	−0.3085(17)	−0.0038(6)	0.7658(17)
C(23)	−0.4184(19)	−0.0483(6)	0.5452(20)
C(30)	−0.1624(16)	−0.0772(6)	0.9362(18)
C(31)	0.0515(18)	−0.0702(7)	1.0366(20)
C(32)	−0.1171(19)	−0.1048(7)	1.1889(18)
C(40)	−0.3394(14)	−0.1167(5)	0.7168(16)
C(41)	−0.4606(16)	−0.1339(6)	0.6441(18)
C(42)	−0.2243(15)	−0.1220(6)	0.6299(18)
C(50)	−0.0982(16)	−0.1366(5)	0.6889(16)
C(51)	0.0124(15)	−0.1303(5)	0.5789(15)
C(52)	0.0375(16)	−0.1638(5)	0.4902(17)
C(53)	0.1420(16)	−0.1621(5)	0.3842(17)
C(54)	0.2161(14)	−0.1280(5)	0.3838(15)
C(55)	0.1886(16)	−0.0935(5)	0.4709(18)
C(56)	0.0814(15)	−0.0971(5)	0.5733(16)
C(57)	0.3328(16)	−0.1252(6)	0.2767(18)
C(60)	−0.0837(16)	−0.1566(5)	0.8143(18)
C(61)	0.0262(16)	−0.1776(5)	0.8801(17)
C(62)	0.0051(17)	−0.2075(6)	0.9870(19)
C(63)	0.1108(18)	−0.2292(6)	1.0538(19)
C(64)	0.2274(19)	−0.2210(6)	1.0181(21)
C(65)	0.2603(18)	−0.1876(6)	0.9155(20)
C(66)	0.1519(17)	−0.1664(6)	0.8503(19)
C(67)	0.3414(22)	−0.2457(8)	1.0894(24)
N(30)	−0.0804(13)	−0.0828(5)	1.0520(14)
O(11)	−0.3896(16)	−0.1634(5)	1.1102(20)
O(12)	−0.6516(12)	−0.0762(5)	0.8713(15)
O(13)	−0.3709(15)	−0.0201(6)	1.1648(16)
O(21)	−0.1099(14)	−0.0191(5)	0.4055(14)
O(22)	−0.3304(14)	0.0252(4)	0.8240(14)
O(23)	−0.5052(14)	−0.0461(5)	0.4721(16)
O(30)	−0.1174(9)	−0.0597(3)	0.8215(11)
Ru(1)	−0.3612(1)	−0.0868(-)	0.9241(1)
Ru(2)	−0.2683(1)	−0.0539(-)	0.6659(1)

A fifth band (yellow-brown) is eluted with CH_2Cl_2/petroleum ether (70 : 30). This fraction consists of a yellow oil (155 mg); spectroscopic data indicate this to be a mixture of products containing some $\{\eta^5\text{-}(OC)_3\overline{RuC(Ar)=C(Ar)C(Ar)=C}(Ar)\}\text{-}Ru(CO)_3$, Ar = *p*-tolyl (**4b**) [1b].

*Reaction of (*p*-anisyl)C≡C(*p*-anisyl) (2c) with* $Ru_3\{\mu\text{-}H;\mu\text{-}O{=}CNMe_2\}(CO)_{10}$ *(1).* To a quantity of **1** (1.00 g, 1.52 mmol) in 350 mL petroleum ether, is added 400 mg (1.68 mmol) of **2c** and the mixture stirred under a stream of N_2 at 23° C for 24 h. Solvent volume is reduced to 30 ml in a rotary evaporator and the residue is placed on a silica gel column (Baker Analyzed, 60–200 mesh; 2 cm dia. × 20 cm length). Three fractions are eluted; starting with petroleum ether, a yellow band which contains $Ru_3(CO)_{12}$, (103 mg, 0.16 mmol, 13%) and excess **2c** (82 mg, 0.34 mmol). Continuing with petroleum ether/CH_2Cl_2 (9 : 1), an orange band is obtained consisting of unreacted **1** (180 mg, 0.27 mmol). With petroleum ether/CH_2Cl_2 (4 : 1) a yellow-orange band is eluted consisting of $\overline{Ru_2\{\mu\text{-}O{=}CNMe_2},\mu\text{-}\sigma,\pi\text{-}C(Ar){=}CH(Ar)\}(CO)_6$, Ar = *p*-anisyl, **3c**, and $\{\eta^5\text{-}\overline{Ru(CO)_3C(Ar{=}C(Ar)C(Ar){=}C}(Ar)\}Ru(CO)_3$, Ar = *p*-anisyl, **4c** (795 mg). Separation of the two components was not attempted, but FAB/MS confirmed the presence of each [1b]. A multiplet centered at 679 is seen which can be assigned to (parent ion − 3 H for **3c**). The MASPAN deconvolution routine indicates that the observed multiplet is a mixture of P (3%), P − 3H (59%) and P − 4H (38%). For **4c**, MASPAN analysis of the P − 3(CO) multiplet centered at 764 showed 12% agreement between calculated and measured *m/e* values.

Reaction of $Ru_2(\mu\text{-}O{=}CNMe_2,\mu\text{-}\sigma,\pi\text{-}C(p\text{-}tolyl){=}CH(p\text{-}tolyl)\}(CO)_6$ *(3b) with* $CH_3C{\equiv}CH$. A quantity of **3b** (375 mg, 0.58 mmol) is dissolved in hexane and freeze–thaw degassed. Propyne gas (3.1 mmol, in a tenfold excess) is bubbled into the stirred solution at 23° C which is left to stir for 4 h. At this time the reaction is complete (IR). Solvent is reduced in volume and the residue is eluted from silica gel with CH_2Cl_2/petroleum ether (1 : 4). The major fraction (190 mg, 0.28 mmol) proved to be $Ru_2\{\mu\text{-}O{=}CNMe_2,\mu\text{-}\sigma,\pi\text{-}C(CH_3){=}C(H)C(p\text{-}tolyl){=}CH(p\text{-}tolyl)\}\text{-}(CO)_6$, **5** (48% based on **3b**). Trace amounts (5 mg and 8 mg) of two other components are also eluted, but were not identified. MASPAN analysis for **5** shows a parent-ion at 679, which corresponds to P − 1(CO).

Crystallographic studies

Data collection for 3b. Yellow air and X-ray stable single crystals were grown by gradual cooling of a saturated CH_2Cl_2/hexane (9 : 1) solution to −30 °C. A crystal was glued to the tip of a glass fiber and mounted on a goniometer head of a Huber four-circle automated diffractometer modified at UCLA by C.E. Strouse for operation under control of a VAX 11/750 computer.

Lattice parameters and standard errors were determined by least squares refinement of the angular setting ($9° < 2\theta < 21°$) of 50 Mo-K_α peaks centered on the diffractometer. The refined unit cell parameters and other specifics relevant to the data collection are given in Table 3.

Background for each peak was determined from the peak profile. The intensities of three standard reflections (1,8,0); (2,0,1); (3,4,2) were recorded after every 97 intensity measurements to monitor crystal and diffractometer stability. The variations in the standards were random showing deviations from the respective mean values of less than 2%.

A survey of the complete data set showed systematic absences for reflections (h, 0, l) $h \neq 2n$, and (0,k,0) $k \neq 2n$ consistent with the assignment of the space group shown in Table 2 [9]. The total number of independent reflections measured and range of 2θ are given in Table 3, as well as the number of reflections used in the solution and refinement. All reflections were corrected for Lorentz and polarization effects and converted to $|F_o|$ and $\sigma(|F_o|)$ by means of the CARESS program (see next paragraph for description of computer programs).

Data collection for 5. A single crystal grown from pentane at −30 °C was selected and glued to a thin glass fiber and mounted on a Syntex $P\bar{1}$ automated diffractometer (equipped with scintillation counter and graphite monochromator) with crystal faces (101) and (001) approximately parallel to the instrumental axis. Lattice parameters and standard errors were determined at 298 °C by least-squares refinement of the angular settings of 15 Mo-K_α (λ = 0.7107 Å) peaks at $20 < 2\theta < 27°$ centered on the diffractometer. The refined unit cell parameters and specifics related to data collection are given in Table 3. Background counts were collected from the peak profile. The intensities of three standard reflections, (3,4,3), (4,12,0) and (5,3,2) were recorded after every 97 intensity measurements throughout the data

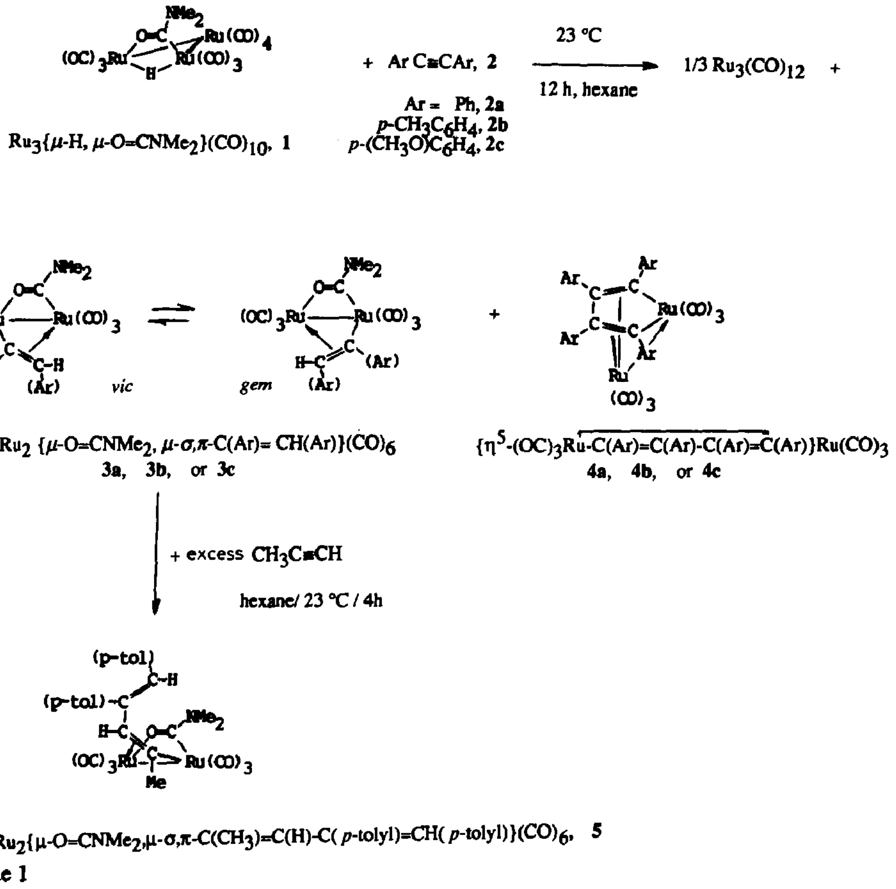

Scheme 1

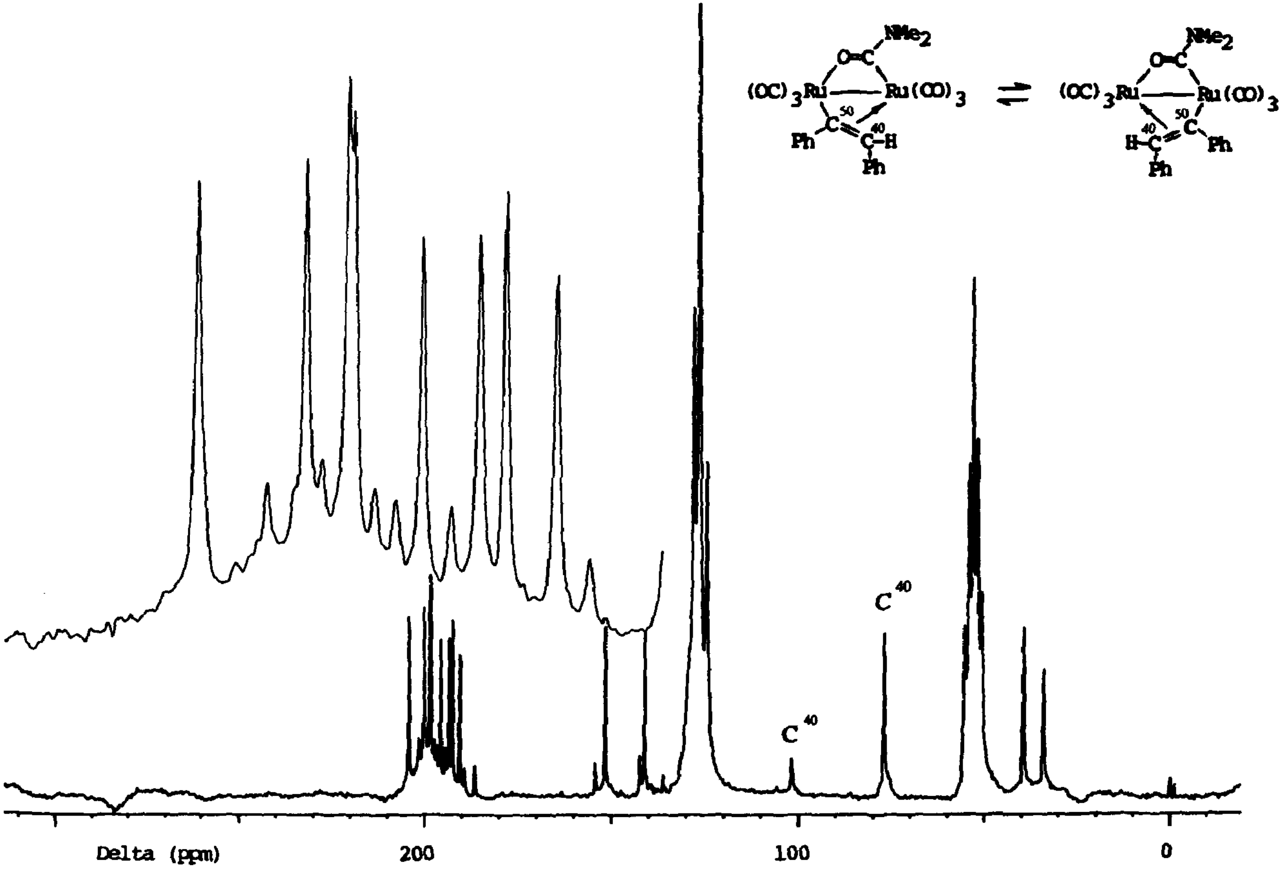

Fig. 1. $^{13}C\{^{1}H\}$ NMR at 22.5 MHz of $Ru_2\{\mu\text{-}O{=}C(NMe_2)\},\mu\text{-}\sigma,\pi\text{-}C(Ph){=}C(H)Ph\}(CO)_6$, 3a, −50 °C, CD_2Cl_2 solution.

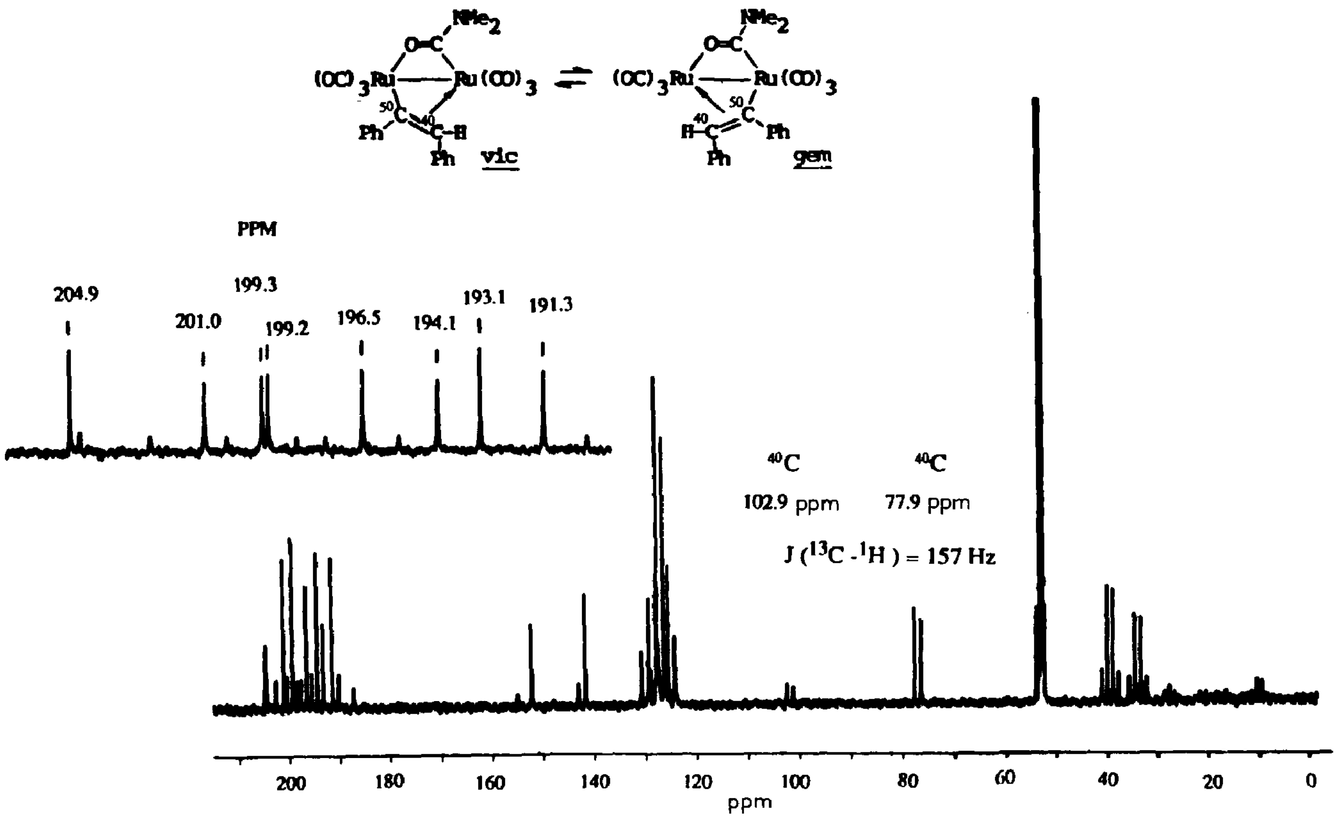

Fig. 2. ^{13}C(^{1}H-coupled) NMR at 125.8 MHz of $Ru_2\{\mu$-$O{=}C(NMe_2),\mu$-σ,π-$C(Ph){=}C(H)Ph\}(CO)_6$, **3a**, −50 °C, CD_2Cl_2 solution. Insert. Peak positions of the resonances of the minor isomer are, respectively: 204.6, 202.6, 200.4, 198.4, 197.6, 195.7, 190.2, 187.1.

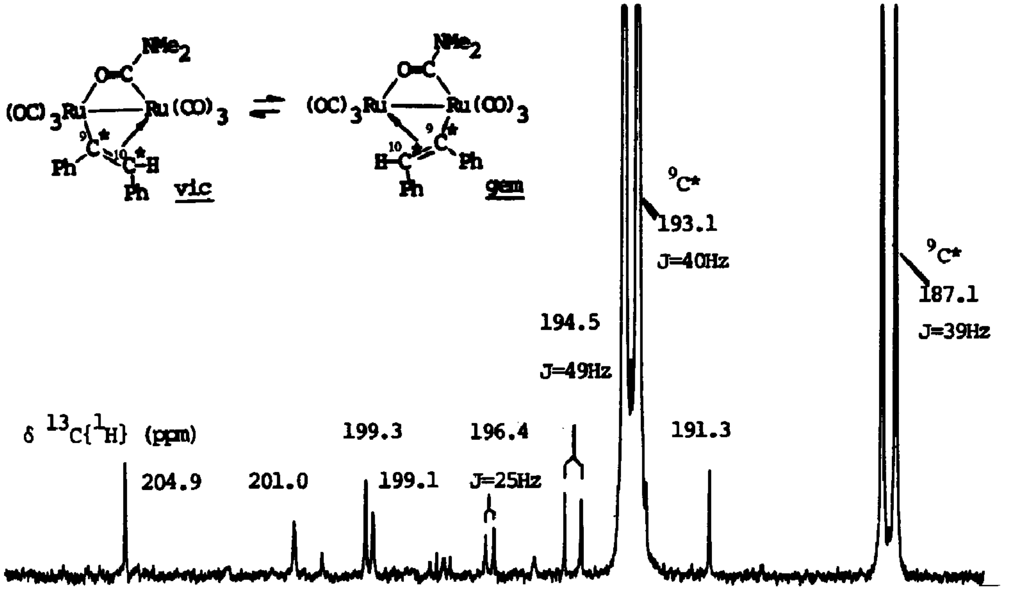

Fig. 3. Carbonyl region, $^{13}C\{^1H\}$ NMR at 125.8 MHz of $Ru_2\{\mu\text{-}O{=}C(NMe_2),\mu\text{-}\sigma,\pi\text{-}^{13}C(Ph){=}^{13}C(H)\text{-}Ph\}(CO)_6$, at −50 °C, CD_2Cl_2 solution showing the ^9C resonance of the vinyl group, reproduced with permission from Supplementary Material of ref. 2. The numbering $(Ph)^9C{=}^{10}C(H)Ph$ of ref. 2 is equivalent to $(Ph)^{50}C{=}^{40}C(H)Ph$ in the present work.

collection to monitor crystal and diffractometer stability. The variations in the standards indicated a decay to about 75% of the original intensities, with a ±2% fluctuation. A survey of the complete data set showed systematic absences for reflections $(0,k,0)$, $k \neq 2n$ $(h,0,l)$, $l \neq 2n$ consistent with the assignment of $P2_1/c$ for the space group.

The total number of independent reflections measured and range of 2θ are given in Table 3, as well as the number of reflections used in the solution and refinement. The observed reflections were corrected for Lorentz and polarization effects and converted to $|F_o|$ and $\sigma(|F_o|)$ by means of the CARESS [10*] program; absorption corrections were not applied (see below).

Solution and refinement of the structures: All calculations were performed on a VAX 11/750 computer (Chemistry Department of UCLA). Programs used for the structure determination consist in all cases of local modifications edited by Dr. C.E. Strouse and his research group [10].

Scattering factors for neutral ruthenium, oxygen and carbon atoms were taken from Table 2.2A of ref. 9 while those for hydrogen were from Stewart et al. [11]. Both real (f') and imaginary (f'') components of anomalous dispersion were included for ruthenium using the values in Table 2.3.1 of ref. 9. The function minimized during least-squares refinement and the discrepancy indices are given in Table 3.

For 3b. Reasonable positions for the metal atoms were obtained using direct methods (MULTAN80). Full-matrix least-squares refinement of the metal atoms with isotropic temperature factors followed by difference Fourier syntheses revealed the

---

* Reference number with asterisk indicates a note in the list of references.

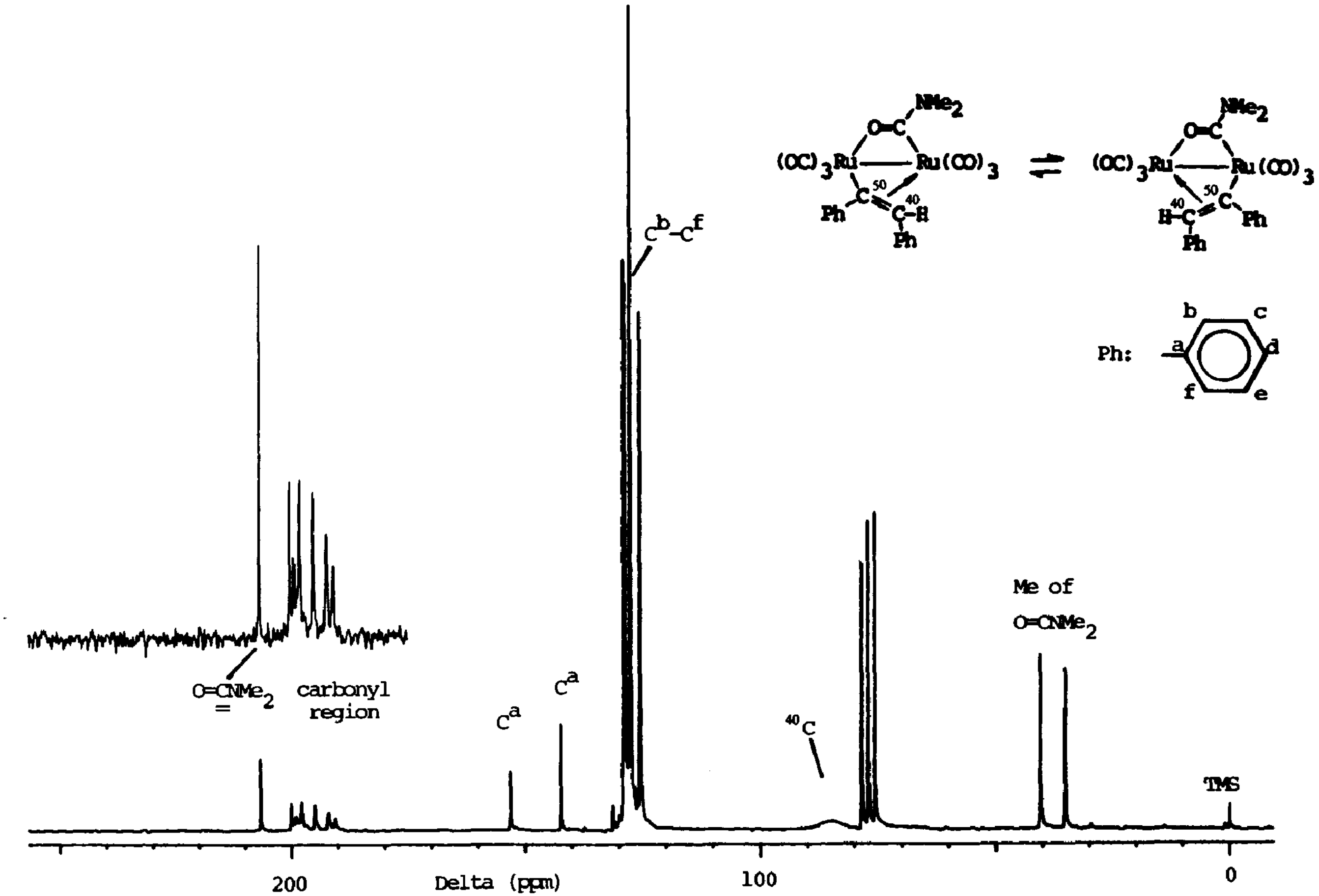

Fig. 4. $^{13}C\{^1H\}$ NMR at 22.5 MHz of $Ru_2\{\mu\text{-}O{=}C(NMe_2),\mu\text{-}\sigma,\pi\text{-}C(Ph){=}C(H)(Ph)\}(CO)_6$, 3a, +30 °C, $CDCl_3$ solution.

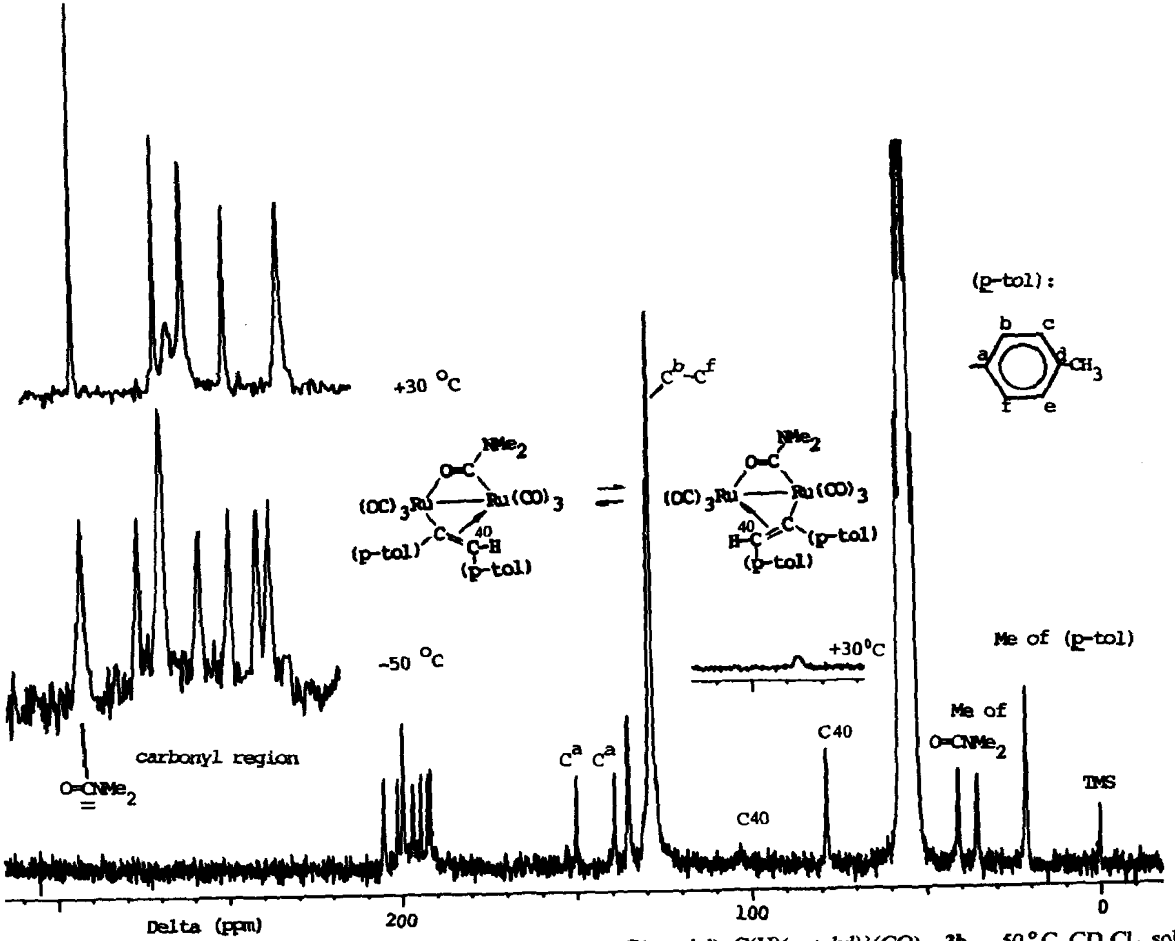

Fig. 5. $^{13}C\{^1H\}$ NMR at 22.5 MHz of $Ru_2\{\mu$-$O{=}C(NMe_2),\mu$-σ,π-$C(p$-tolyl$){=}C(H)(p$-tolyl$)\}(CO)_6$, **3b**, − 50 ° C, CD_2Cl_2 solution with inserts showing selected spectral features at 30 ° C.

positions of other atoms and, after further refinement, the positions of all non-hydrogen atoms. The data were also corrected for the effects of absorption, see Table 3. Least-squares refinement first with anisotropic thermal parameters for all the metal atoms and then, with anisotropic thermal parameters for all non-hydrogen atoms, afforded the *R* factors shown in Table 3.

Table 6

Selected interatomic distances (Å) and angles (deg) for $Ru_2\{\mu$-O=CNMe$_2$,μ-σ,π-C(*p*-tolyl)=CH(*p*-tolyl)$\}(CO)_6$, **3b**

Ru(01)–Ru(02)	2.739(1)	Ru(01)–C(40)	2.336(6)
Ru(01)–C(30)	2.106(7)	Ru(01)–C(50)	2.324(7)
Ru(02)–O(30)	2.117(5)	Ru(02)–C(50)	2.081(7)
C(30)–O(30)	1.283(8)	C(40)–C(50)	1.410(9)
C(30)–N(30)	1.340(9)	C(40)–H(40A)	1.182
N(30)–C(31)	1.474(10)	C(40)–C(41)	1.498(9)
N(30)–C(32)	1.456(11)	C(50)–C(51)	1.504(9)
O(30)–C(30)–N(30)	115.05(65)	C(40)–C(50)–C(51)	118.81(63)
O(30)–C(30)–Ru(01)	113.88(46)	C(40)–C(50)–Ru(02)	119.74(50)
N(30)–C(30)–Ru(01)	131.06(56)	C(40)–C(50)–Ru(01)	72.87(38)
C(30)–O(30)–Ru(02)	99.68(41)	C(51)–C(50)–Ru(02)	120.94(48)
		C(51)–C(50)–Ru(01)	128.58(47)
H(40A)–C(40)–C(41)	113.31	Ru(02)–C(50)–Ru(01)	76.69(22)
H(40A)–C(40)–Ru(01)	98.90		
C(50)–C(40)–C(41)	125.23(63)		
C(50)–C(40)–Ru(01)	71.91(37)		
C(41)–C(40)–Ru(01)	123.84(47)		

Table 7

Selected interatomic distances (Å) and angles (deg) for $Ru_2\{\mu$-O=CNMe$_2$,μ-σ,π-C(CH$_3$)=C(H)C(*p*-tolyl)$\}(CO)_6$, **5**

Ru(01)–Ru(02)	2.725(2)	Ru(01)–C(40)	2.107(15)
Ru(01)–C(30)	2.098(18)	Ru(02)–C(40)	2.257(17)
Ru(02)–O(30)	2.098(10)	Ru(02)–C(42)	2.327(19)
C(30)–O(30)	1.266(19)	C(40)–C(42)	1.442(20)
C(30)–N(30)	1.347(19)	C(40)–C(41)	1.586(22)
N(30)–C(31)	1.444(21)	C(42)–C(50)	1.493(22)
N(30)–C(32)	1.472(21)	C(50)–C(60)	1.306(20)
O(30)–C(30)–N(30)	116.30(158)	C(42)–C(40)–C(41)	114.60(139)
O(30)–C(30)–Ru(01)	113.48(118)	C(42)–C(40)–Ru(01)	128.39(123)
N(30)–C(30)–Ru(01)	129.78(124)	C(42)–C(40)–Ru(02)	74.32(98)
C(30)–O(30)–Ru(02	107.10(101)	C(41)–C(40)–Ru(01)	116.96(97)
		C(41)–C(40)–Ru(02)	122.11(120)
C(50)–C(42)–Ru(02)	116.11(121)	Ru(02)–C(40)–Ru(01)	77.22(57)
C(60)–C(50)–C(42)	124.21(146)		
C(60)–C(50)–C(51)	122.12(155)		
C(42)–C(50)–C(51)	113.30(131)		
C(50)–C(60)–C(61)	132.17(150)		

At this stage, it was possible to locate all hydrogen atoms as follows: the position of the vinyl hydrogen atom (H40a) was found on a difference electron density map. At least one hydrogen atom on each of the four methyl groups was located and, using these positions, the twelve methyl hydrogen atoms were fixed in calculated positions with C–H = 1.00 Å and H–C–H = 109.5°. The hydrogen atoms of the phenyl rings were fixed in calculated positions with C–H = 1.00 Å. Neither the positions nor the temperature factors (assigned to be $B = 7$ or 8) for all hydrogen atoms were refined; the parameters were used only for calculation of the final structure factors given in Table 3. Atomic positional parameters are given in Table 4.

For 5. The solution for the structure was obtained by a straightforward application of the heavy-atom method that quickly yielded reasonable positions for the two ruthenium atoms. Full-matrix least squares refinement on the metal atoms followed by difference Fourier syntheses revealed positions of all non-hydrogen atoms. Least squares refinement for all non-hydrogen atoms, all anisotropic with the exception of tolyl-carbon atoms afforded R factors and GOF shown in Table 3. Hydrogen atoms were not located. Highest peaks on a final difference map correspond to 1 $e^-/Å^3$ and are near ruthenium atoms. The final atomic position and thermal parameters are given in Table 5.

Results

The synthesis of the σ,π-vinyl complexes is summarized in Scheme 1. The new complexes, **3a**, **3b**, and **3c**, are the principal products of the reaction, accompanied by the previously known metallacyclic derivatives as principal by-products [8]. IR and NMR data are given in Tables 1 and 2. $^{13}C\{^1H\}$ NMR spectra of the new complexes were obtained over the temperature range −50 to +30°C. $^{13}C\{^1H\}$ and ^{13}C(H-coupled) spectra for **3a** at −50°C are shown in Figs. 1 and 2, respectively; Figure 3 will be introduced in the Discussion. A $^{13}C\{^1H\}$ spectrum for **3a** at 30°C is shown in Fig. 4. $^{13}C\{^1H\}$ spectra for **3b** at two different temperatures are shown in Fig. 5. Selected interatomic distances and angles relating to the crystal structures for **3b** and **5** are given in Tables 6 and 7, respectively.

Discussion

^{13}C NMR spectra. The limiting $^{13}C\{^1H\}$ spectrum of **3a** at −75°C shows broadening of all resonances due to onset of crystallization in the NMR tube; at −50°C (Fig. 1) the principal resonances are observed to be accompanied by a closely matching set of weaker peaks. This indicates two isomers in solution in unequal population, namely *vic* or *gem* referring to the two different possible attachments of the μ-σ,π-vinyl group shown in the structures on Fig. 1 or 2. The two peaks labelled ^{40}C are identified as belonging to the =*C*(H)Ph of the μ-σ,π-vinyl group in the two isomers by the appearance of these peaks as doublets in the $^{13}C(^1H$-coupled) spectrum (Fig. 2). By the same token, the singlet appearance of the resonances between 160 and 140 ppm are assigned as the *ipso*-carbon atoms of the phenyl rings by their persistence as singlets in the ^1H-coupled spectrum (Fig. 2).

Eight major resonances are observed in the carbonyl region (δ = 185–210 ppm, see inserts in Figs. 1 and 2). Six of these correspond to the six terminally bonded

Table 8

Comparison of ^{13}C chemical shifts for the μ-σ,π-vinyl group [a]

Compound [b]	$\delta(C^1)$	$\delta(C^2)$
$Os_3(CO)_{10}(\mu\text{-}I)\{\mu\text{-}C^1(OCH_3){=}C^2H_2\}$ [d]	199.4	35.9
$Fe_2(CO)_6(\mu\text{-}SC_2H_5)(\mu\text{-}C^1H{=}C^2H_2)$ [e]	157.2	73.9
$Os_3(CO)_{10}(\mu\text{-}H)\{\mu\text{-}C^1H{=}C^2(H)CHMe_2\}$ [f]	112.48 and 95.8 [c]	
$Ru_2W(CO)_3\{\mu\text{-}\sigma,\pi\text{-}trans\text{-}C^1H{=}C^2(R)H\}(\mu\text{-}CO)(\eta^5\text{-}C_5H_5)_3$ [g]		
R = *p*-tolyl	142.7	142.3
R = Me	147.1	76.1
$(\eta^5\text{-}C_5Me_5)Ru(CH_2{=}CH_2)(\mu\text{-}C^1H{=}C^2H_2)_2Ru(\eta^5\text{-}C_5Me_5)$ [h]	188.5	54.5
$(\eta^5\text{-}C_5Me_5)Ru(NO)(CH_3)(C^1H{=}C^2H_2)$ [i]	156.89	120.36
$(\eta^5\text{-}C_5H_5)Ru(PPh_3)_2\{(E)\text{-}C(CO_2Me){=}C(CO_2Me)H\}$ [j]	182.2	163.0
$(\eta^5\text{-}C_5H_5)Fe\{P(OPh)_3\}\{C^1(R){=}C^2(Ph)Me\}$		
R = Me, *E* configuration [k]	137.7	149.1
R = Me, *Z* configuration [k]	136.5	152.4
R = Ph, *Z* configuration [l]	157.0	157.2
$(\eta^5\text{-}C_5H_5)Fe(CO)_2(CH{=}CHCH_2CH_2CH_3)$ [m]	145.7 and 124.0 [c]	
$Ru_2\{\mu\text{-}O{=}C(NMe_2,C(Ph){=}C(Ph)H\}(CO)_5L$ [n]		
L = CO, (*vic*) [o]	187.4	102.9
L = CO, (*gem*) [o]	193.5	77.9
L = PPh_3, (*vic*)	186.0	97.8
L = PPh_3, (*gem*)	197.6	76.3

[a] Reproduced with permission from the Supplementary Material of ref. 2. [b] $M(\mu\text{-}\sigma,\pi\text{-}C^1R{=}C^2R'R''\}M'$. [c] C^1 and C^2 are not distinguished. [d] S.L. Bassner, E.D. Morrison, G.L. Geoffroy, Organometallics, 6 (1987) 2207. [e] D. Seyferth, C.M. Archer, Organometallics, 5 (1986) 2572. [f] M. Green, A.G. Orpen, C.J. Schaverien, J. Chem. Soc., Chem. Commun. (1984) 37. [g] D.L. Davies, M.J. Parrott, P. Sherwood, F.G.A. Stone, J. Chem. Soc., Dalton Trans. (1987) 1201. [h] H. Suzuki, H. Omori, Y. Moro-Oka, Organometallics, 7 (1988) 2579. [i] J. Chang, R.G. Bergman, J. Am. Chem. Soc., 109 (1987) 4298. [j] M.I. Bruce, A. Catlow, M.G. Humphrey, G.A. Koutsantonis, M.R. Snow, E.R.T. Tiekink, J. Organomet. Chem., 338 (1988) 59. [k] D.L. Reger, K.A. Belmore, E. Mintz, N.G. Charles, E.A.H. Griffith, E.L. Amma, Organometallics, 2 (1983) 101. [l] D.L. Reger, E. Mintz, L. Lebioda, J. Am. Chem. Soc., 108 (1986) 1940. [m] C.P. Casey, S.R. Marder, R.E. Colborn, P.A. Goodson, Organometallics, 5 (1986) 199. [n] See Table III of ref. 2; L = CO, 3, L = PPh_3, 4; $C^1 = C^9$, and $C^2 = C^{10}$. [o] Equivalent to data for **3a** this work, see Table 2 and Figs. 1–3.

CO groups and the seventh to the acyl carbon of the bridging carboxamido group. The eight resonance must therefore belong to ^{50}C of the μ-σ,π-vinyl group. However, none of the ^{1}H-coupled resonances (see insert in Fig. 2) shows doubling, due to the fact that the coupling constant $^2J(^1H\text{-}C{=}^{13}C)$ is close to zero [12]. The ^{50}C resonance was identified by ^{13}C enrichment, see Fig. 3 [2]. Two doublets (due to $^{13}C\text{-}^{13}C$ coupling) are seen in the NMR spectrum of the complex containing the ^{13}C-enriched diphenylacetylene, one belonging to ^{50}C of the major isomer, and the other belonging to the corresponding resonance in the minor isomer. In the PPh_3-substituted derivatives [2], the isomers could be assigned due to additional $^{31}P\text{-}^{13}C$ coupling, the principal component of the equilibrium mixture in solution being the *gem* isomer. A similar assignment is assumed for the unsubstituted isomers, but is not confirmed by the data at hand. A comparison of ^{13}C chemical shifts for the carbon atoms of the bridging sigma–pi vinyl group is given in Table 8.

The two sets of signals each for ^{50}C and ^{40}C are observed to *merge* at +30 °C giving a single set of resonances at the population-weighted chemical shift average positions, see Fig. 4. Fluxionality is thus indicated between the *gem* and *vic* isomers. A similar pattern of two sets of resonances at −50 °C merging to a single

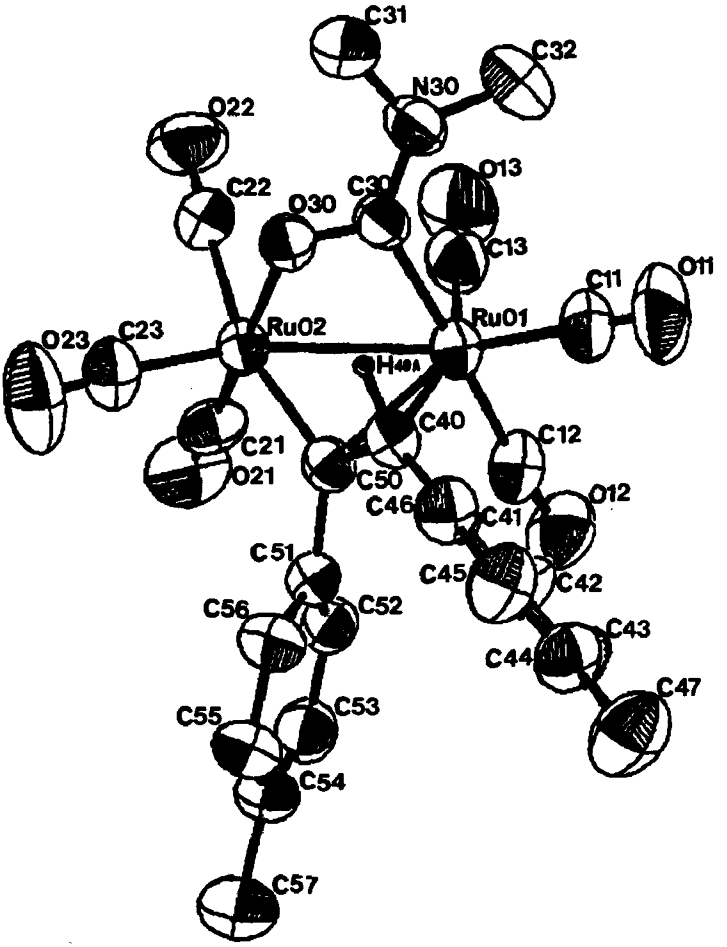

Fig. 6. ORTEP projection of $Ru_2\{\mu\text{-}O{=}C(NMe_2),\mu\text{-}\sigma,\pi\text{-}C(p\text{-tolyl}){=}C(H)(p\text{-tolyl})\}(CO)_6$, **3b**; thermal ellipsoids at 50% probability.

set at +30 °C is seen for **3b**, Fig. 5. Fluxionality of μ-σ,π-vinyl complexes has been reported for the trinuclear osmium compounds $HOs_3(CO)_{10}(CH{=}CH_2)$ [4] and $HOs_3(CO)_{10}(CPh{=}CPh_2)$ [5]. However, this averaging could be observed only through changes in the carbonyl resonances; due to symmetry in these complexes the resonances of the μ-σ,π-vinyl groups are unchanged in the tautomers. Since these early observations, tautomerism of μ-σ,π-vinyl complexes has also been observed in some di-rhenium [13a] and di-iron [13b–d] complexes.

Structure of complex 3b. The crystal consists of discrete molecules of $Ru_2\{\mu\text{-}O{=}CNMe_2,\mu\text{-}\sigma,\pi\text{-}C(p\text{-}CH_3C_6H_4){=}CH(p\text{-}CH_3C_6H_4)\}(CO)_6$, separated by normal van der Waals distances. A view of the complex and the system for labelling the atoms is shown in Fig. 6, and selected interatomic distances and angles are presented in Table 6. More extensive listings of bond distances and angles are available with the supplementary material.

The molecule is a double bridged dimer where the two bridging groups, namely $\{\mu\text{-}\sigma,\pi\text{-}C(p\text{-}CH_3C_6H_4){=}CH(p\text{-}CH_3C_6H_4)\}$ and $\{\mu\text{-}O{=}CNMe_2\}$, are seen to be attached to the two metal centers in a *vicinal* arrangement; the metal–metal separation with 2.739(1) Å is slightly longer than in the *gem* bis-acyl derivative Ru$_2${μ-O=C(Et)$_2$}(CO)$_6$ [14].

The vinyl ligand interacts with both ruthenium atoms: it is σ-bonded to Ru2 [Ru2–C50 = 2.081(7) Å] and π-bonded to the Ru1 [Ru1–C40 = 2.336(6) Å and Ru1–C50 = 2.324(7) Å]. Consistent with the structural feature of a π-bonded alkene with a carbon–ruthenium bond in place of one hydrogen or organic group is the bond length of the multiple bond [C50–C40 = 1.410(9) Å]. This is ca. 0.09 Å longer than expected for a normal C=C bond and similar to values found in other σ,π-vinyl clusters like HOs$_3$(CO)$_{10}$(PhC=CHPh), 1.40(5) Å, [5] and FeCO$_3$(CO)$_9$(PhC=CHPh)(PhC$_3$Ph), 1.42(2) Å [16].

The *p*-tolyl groups exhibit *cis* coordination as expected for the insertion of acetylene into a metal–hydrogen bond and the angles around C50 and C40 show only a slight deviation from the ideal 120° angle in an sp^2 carbon.

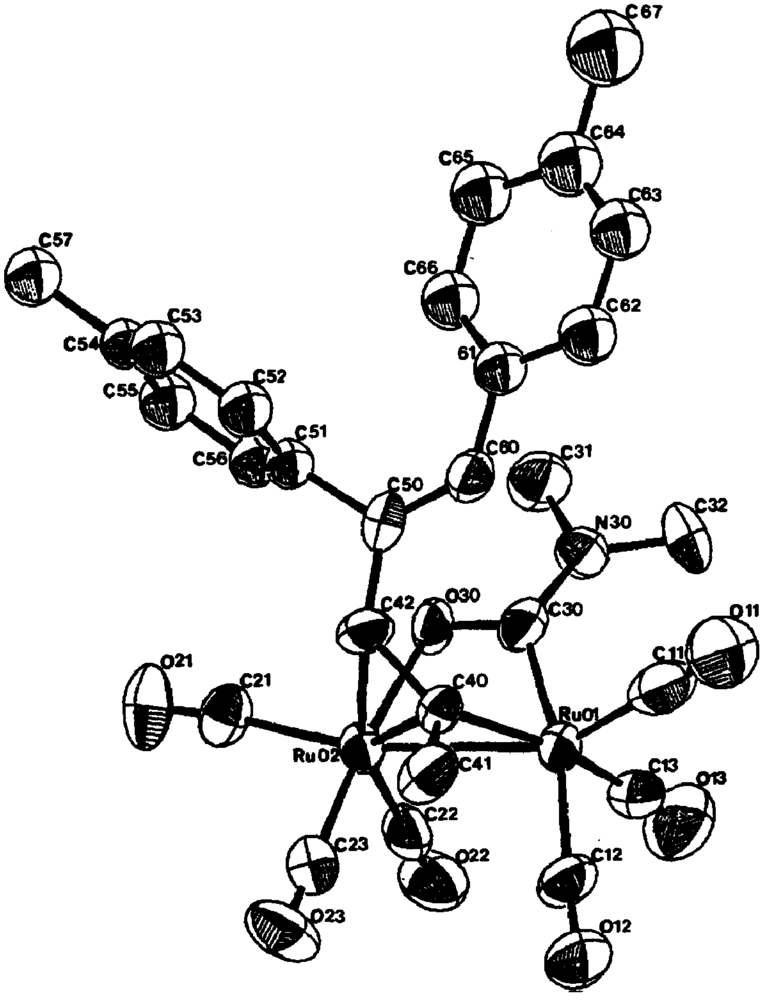

Fig. 7. ORTEP projection of Ru$_2${μ-O=CNMe$_2$,μ-σ,π-C(CH$_3$)=C(H)C(*p*-tolyl)=CH(*p*-tolyl)}(CO)$_6$, 5; thermal ellipsoids at 50% probability.

Within the carboxamido group the C–O and the C–N separations are 1.283(8) and 1.34(9) Å, respectively. Comparison with standard bond lengths of $C(sp^2) = O = 1.20$ Å and $C(sp^2)\text{–}N = 1.43$ Å [15] indicates delocalized bonding along the O–C–N frame. The Ru1–C30 distance of 2.106(7) Å and the Ru2–O30 separation of 2.117(5) Å are in the range expected for this bridging ligand. The structural features are similar to those in the starting complex **1** [17] and in the monosubstituted derivative $Ru_3\{\mu\text{-H},\mu\text{-O=CNMe}_2\}(CO)_9P(OPh)_3$ [18].

Structure of complex 5. The crystal consists of discrete molecules of $Ru_2\{\mu\text{-O=CNMe}_2,\mu\text{-}\sigma,\pi\text{-C(CH}_3\text{=CHC(}p\text{-tolyl)=CH(}p\text{-tolyl)}\}(CO)_6$, separated by normal van der Waals distances. The two metals in this complex are also found to be doubly bridged, but with these groups bonded in a *geminal* configuration. A view of the complex and the system for labelling the atoms is shown in Fig. 7. A crystal packing diagram viewed down the *b* axis is available as Supplementary Material. The principal interactions are between adjacent rows of molecules, i.e. between *p*-tolyl groups on one side and between carbonyl groups on the other side. Selected interatomic distances and angles are presented in Table 7. A more extensive listing of bond distances and angles is available as Supplementary Material.

The Ru–Ru separation of 2.726(2) Å is slightly shorter than for structure **3b**, and similar to that seen in a variety of bridged ruthenium dimers, such as $Ru_2\{\mu\text{-X}\}_2(CO)_4L_2$, L = P(t-Bu)$_3$ (X = Br, Ru–Ru = 2.672(2) Å; X = OBu, Ru–Ru = 2.728(2) Å [19a,b]. It also compares well with another *geminal* ruthenium dimer reported from this research group of $Ru_2\{\mu\text{-O=C(Et)}\}_2(CO)_6$ of 2.686 Å [14].

Except for the *geminal* positioning of the bridging groups in **5**, the features within the σ,π-vinyl and carboxamido group follow in an analogous fashion as discussed above for **3b**. Within the 1,3-butadienyl σ,π-C(Me)=C(H)C(Ph)=C(H)Ph group, the central bond C(42)–C(50) = 1.493(22) Å. This shortness (standard $C(sp^2)\text{–}C(sp^2) = 1.480$ Å, $C(sp^2)\text{–}C(sp^3) = 1.520$ Å [15]) indicates some delocalization of electrons. For the coordinated π-bond the C(40)–C(42) distance is comparable to that in other complexes indicated in Table 9.

Supplementary Material is available in the Dissertation of W. Krone-Schmidt [1b]. For the derivatives **1**, **3a**, **3b**, **3c**, **4a**, **4b**, **4c**, and **5**: MASPAN calculations for

Table 9

Comparison of structural data (Å) for the μ-σ,π-vinyl group

Compound [a]	M–C^1	M′–C^1	M′–C^2	C=C
$FeCo_3(CO)_9(Ph_2C_2)\{\mu\text{-C}^1\text{(Ph)=C}^2\text{(H)Ph}\}$ [b]	1.981(11)	1.996(10)	2.127(11)	1.42(2)
$Os_3(CO)_{10}\{\mu\text{-H},\mu\text{-C}^1\text{(Ph)=C}^2\text{(H)Ph}\}$ [c]	2.11(4)	2.34(4)	2.44(4)	1.40(5)
	2.18(4)	2.21(4)	2.45(4)	1.31(5)
$Os_3(CO)_{10}\{\mu\text{-H},\mu\text{-C}^1\text{(H)=C}^2\text{(H)CMe}_3\}$ [d]	2.10(2)	2.27(2)	2.43(2)	1.38(4)
$Os_3(CO)_{10}\{\mu\text{-H},\mu\text{-C}^1\text{(H)=C}^2\text{(H)Et}\}$ [e]	2.15(2)	2.28(2)	2.46(3)	1.40(3)
$Os_3(CO)_{10}\{\mu\text{-H},\mu\text{-C}^1\text{(H)=C}^2\text{H}_2\}$ [f]	2.107(3)	2.273(3)	2.362(3)	1.396(3)
$Ru_2\{\mu\text{-O=C(NMe}_2\text{,C(Ph)=C(Ph)H}\}(CO)_5PPh_3$ [g]	2.085(6)	2.327(6)	2.329(6)	1.416(9)
$Ru_2\{\mu\text{-O=C(NMe}_2\text{,C(Ph)=CH}_2\}(CO)_5PPh_3$ [g]	2.130(6)	2.319(5)	2.331(6)	1.396(8)
3b (this work)	2.081(7)	2.324(7)	2.336(6)	1.410(9)
5 (this work)	2.107(15)	2.257(17)	2.327(19)	1.442(20)

[a] $M\{\mu\text{-}\sigma,\pi\text{-C}^1\text{R=C}^2\text{R}'\text{R}''\}M'$. [b] Ref. 15. [c] Ref. 5. [d] E. Sappa, A. Tiripicchio, A.M. Manotti-Lanfredi, J. Organomet. Chem., 249 (1983) 391. [e] J.J. Guy, B.E. Reichert, G.M. Sheldrick, Acta Crystallogr., B32 (1976) 3319. [f] A.G. Orpen, A.V. Rivera, E.G. Bryan, D. Pippard, G.M. Sheldrick, K.D. Rouse, J. Chem. Soc., Chem. Commun. (1978) 723. [g] Ref. 2.

parent ion peaks, carbonyl IR absorptions, ^{1}H NMR spectra [1b]. For the structures of **3b** and **5**: Tables of thermal parameters and hydrogen atom positions; complete Tables of bond angles and distances, views of the packing diagrams of the unit cells, and calculated and observed structure factors.

Conclusions. The structures described here have revealed connectivity of the organic groups on two dinuclear frameworks. The *vic* isomer is the one observed for **3b** in the solid. It may, however, not be the prevalent isomer in solution, cf. finding of the *gem* isomer to predominate in solution for the substituted complex $Ru_2\{\mu\text{-}O{=}CNMe_2,\mu\text{-}\sigma,\pi\text{-}C(Ar){=}CH(Ar)\}(CO)_5(PPh_3)$, while the *vic* isomer is the one obtained in the solid [2]. Owing to the fluxional behavior for the σ–π bonded group, whatever the prevalent isomer for **3b** may be in solution, it would reflect the thermodynamic preference of the product rather than the kinetic path for the initial insertion reaction. It is interesting to note that after one homologation with MeC_2H, the next product shows *geminal* preference (in the solid). There is not much energy difference between the *geminal* or *vicinal* isomers based on the coalescence of the peaks of the two constituents at +30 °C. Perhaps the steric effects between the enlarged organic group and the methyl groups of $\{\mu\text{-}O{=}CNMe_2\}$ may be responsible for this difference.

Complex **5** is formally related to the metallocyclic derivatives **4a**, **4b**, **4c** by loss of a molecule of dimethylformamide, indicated by the transformation **A** to **C** in Scheme 2. We have not had the opportunity to test this transformation directly; complex **5** in the present work represented by **A** in Scheme 2, differs in the groups R and R′ from *C*, in which R = R′ = R″ (in **4**). The isolated complex **5** is also formally related to complex **B** in Scheme 2 by migration of the (C(R)=C(R′)CR″ = CR″) group onto a coordinated CO, which becomes a *vicinally* bonded bridging acyl group. A complex like **B** in which $R = R' = R'' = CH_3$ was characterized in a previous study [1a]. The chain growth on the sigma–pi vinyl derivative **3** to give the unsaturated organic polyene complex **5** contrasts with an alternating M–H and CO insertion sequence in the complex $[Fe_2(CO)_6\{\mu\text{-}C(C(O)OCH_3)\}C(C(O)OCH_3C(O)\text{-}$

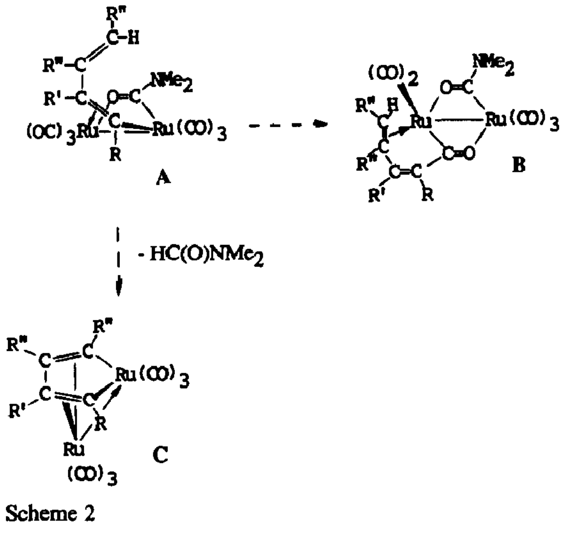

Scheme 2

$C(C_6H_5)C(C_6H_5)H)]^-$, obtained in reactions of acetylenes with a tri-iron system [20].

Acknowledgment

This work was supported by the National Science Foundation (Grant CHE-84-05517), a NATO Fellowship from the DAAD (German Academic Exchange Service) to W.J. Sieber, and a NATOSERC Fellowship to N.M. Boag. The assistance of Mr. Ziling Xue in preparation of Table 9 and Fig. 3 [2] is gratefully acknowledged.

References

1 (a) N.M. Boag, W.J. Sieber, C.E. Kampe, C.B. Knobler, H.D. Kaesz, J. Organomet. Chem., 355 (1988) 385; (b) Taken in part from the Ph.D. Dissertation of W. Krone-Schmidt, UCLA, 1985; (c) This work was reported in preliminary form in an invited lecture presented at the 25th International Conference on Coordination Chemistry held in Nanjing, China: 26–31 July 1987: H.D.Kaesz, Z. Xue, Y.-J. Chen, C.B. Knobler, W. Krone-Schmidt, W.J. Sieber, N.M. Boag, Pure Appl. Chem., 60 (1988) 1245.

2 (a) Z. Xue, W.J. Sieber, C.B. Knobler, and H.D. Kaesz, J. Am. Chem. Soc., 112 (1990) 1825; (b) Ph.D. Dissertation of Z. Xue, UCLA, 1989.

3 (a) Y.-J. Chen, Ph.D. Dissertation, UCLA, 1986; (b) O. Gambino, G.A. Vaglio, R.P. Ferrari, G. Cetini, J. Organomet. Chem., 30 (1971) 381.

4 (a) A.J. Deeming, S. Hasso, M. Underhill, J. Organomet. Chem., 80 (1974) C53, and J. Chem. Soc., Dalton Trans., (1975) 1614; (b) J.R. Shapley, S.I. Richter, M. Tachikawa, J.B. Keister, J. Organomet. Chem., 94 (1975) C43.

5 D.D. Clauss, M. Tachikawa, J.R. Shapley, C.G. Pierpont, Inorg. Chem., 20 (1981) 1528.

6 A.C. Cope, D.S. Smith, R.J. Cotter, Organic Syntheses Coll. Vol. IV, McGraw Hill, New York, 1963, p. 377.

7 N.M. Boag, C.E. Kampe, Y.-C. Lin, H.D. Kaesz, Inorg. Chem., 21 (1982) 1706.

8 (a) C.T. Sears, Jr., F.G.A. Stone, J. Organomet. Chem., 11 (1968) 644; (b) O. Gambino, G. Cetini, E. Sappa, M. Valle, J. Organomet. Chem., 20 (1969) 195; (c) G. Cetini, O. Gambino, E. Sappa, M. Valle, J. Organomet. Chem., 17 (1969) 437.

9 International Tables for X-Ray Crystallography, Vol. IV, Kynoch Press, Birmingham, 1975.

10 UCLA crystallographic package consisting of locally-written or modified versions of the following programs: for data reduction, CARESS, originally written by R.W. Broach (Univ. of Wisconsin) and P. Coppens, P. Becker and R.H. Blessing (SUNY, Buffalo NY); Patterson and Fourier summations, and for statistical methods, MULTAN80, P. Main et al. (Univ. of York); for full matrix least-squares and error analysis, ORFLS and ORFFE, W.R. Busing, K.O. Martin and H.A. Levy (Oak Ridge National Lab., TN); for absorption correction, ABSN, P. Coppens; for least-square planes, MG84, P. Gantzel and K.N. Trueblood; for thermal ellipsoid plot program ORTEP II, C.K. Johnson (Oak Ridge National Lab. TN); for structure factor table listing, PUBLIST, E. Hoel.

11 R.F. Stewart, E.R. Davidson, W.T. Simpson, J. Chem. Phys., 42 (1965) 3175.

12 J.L. Marshall, Carbon–Carbon and Carbon–Proton NMR Couplings, in A.P. Marchand (Ed.), Methods in Stereochemical Analysis, Vol. 2, 1983, p. 33.

13 (a) K.-H. Franzreb and C.G. Kreiter, Z. Naturforsch. B, 37 (1982) 1058; (b) S.C. Kao, P.Y. Lu and R. Pettit, Organometallics, 1 (1982) 911; (c) A.F. Dyke, S.A.R. Knox, M.J. Morris, P.J. Naish, J. Chem. Soc., Dalton Trans. (1983) 1417; (d) C.P. Casey, S.R. Marder, B.R. Adams, J. Am. Chem. Soc., 107 (1985) 7700.

14 C.E. Kampe, N.M. Boag, H.D. Kaesz, J. Mol. Catal. 21 (1983) 297.

15 Interatomic Distances Supplement, Special Publication No. 18, The Chemical Society, London, 1965.

16 S. Aime, D. Osella, L. Milone, A.M. Manoti Lanfredi, A. Tiripicchio, Inorg. Chim. Acta, 71 (1983) 141.

17 R. Szostak, C.E. Strouse, H.D. Kaesz, J. Organomet. Chem., 191 (1980) 243.

18 A. Mayr, Y.-C. Lin, N.M. Boag, C.E. Kampe, C.B. Knobler, H.D. Kaesz, Inorg. Chem., 23 (1984) 4640.

19 (a) H. Schumann, J. Opitz, J. Pickardt, Chem. Ber., 113 (1980) 1385; (b) H. Schumann, J. Opitz, J. Pickardt, J. Organomet. Chem., 128 (1977) 253.
20 J. Ros, X. Solans, M. Font-Altaba, R. Mathieu, Organometallics, 3 (1984) 1014.